AGU ADVANCING EARTH AND SPACE SCIENCE

JGR Atmospheres

RESEARCH ARTICLE

10.1029/2020JD033263

Key Points:

- First implementation of the Model of Emissions of Gases and Aerosols from Nature (MEGAN) model drought response for investigating China air quality
- The drought scheme considering both mild and severe drought improves the model performance in severe drought-hit regions
- Prominent changes of O_3 (−8%) and secondary organic aerosols (SOA) (−30%) are predicted in the drought year in southern China

Supporting Information:

Supporting Information may be found in the online version of this article.

Correspondence to:

P. Wang and T. Wang,

peng.ce.wang@polyu.edu.hk;

tao.wang@polyu.edu.hk

Citation:

Wang, P., Liu, Y., Dai, J., Fu, X., Wang, X., Guenther, A., & Wang, T. (2021). Isoprene emissions response to drought and the impacts on ozone and SOA in China. *Journal of Geophysical Research: Atmospheres*, *126*, e2020JD033263. https://doi.org/10.1029/2020JD033263

Received 8 JUN 2020

Accepted 13 MAR 2021

Author Contributions:

Conceptualization: Peng Wang, Alex Guenther

Data curation: Peng Wang, Yiming Liu, Jianing Dai

Formal analysis: Peng Wang, Yiming Liu, Xiao Fu

Funding acquisition: Tao Wang

Investigation: Peng Wang, Yiming Liu, Jianing Dai

Methodology: Peng Wang, Alex Guenther, Tao Wang

Project Administration: Peng Wang, Tao Wang

Software: Peng Wang, Yiming Liu, Jianing Dai, Xiao Fu

Supervision: Tao Wang

Validation: Peng Wang, Yiming Liu

Isoprene Emissions Response to Drought and the Impacts on Ozone and SOA in China

Peng Wang[1], Yiming Liu[1,2], Jianing Dai[1], Xiao Fu[1,3], Xuemei Wang[4], Alex Guenther[5], and Tao Wang[1]

[1]Department of Civil and Environmental Engineering, Hong Kong Polytechnic University, Hong Kong, China, [2]now at School of Atmospheric Sciences, Sun Yat-sen University, Zhuhai, China, [3]now at Institute of Environment and Ecology, Tsinghua Shenzhen International Graduate School, Tsinghua University, Shenzhen, China, [4]Institute for Environmental and Climate Research, Jinan University, Guangzhou, China, [5]Department of Earth System Science, University of California, Irvine, CA, USA

Abstract Among the various environmental factors that affect isoprene emissions, drought has only been given limited attention. Four different drought response (DR) schemes were implemented in the Model of Emissions of Gases and Aerosols from Nature (MEGAN, version 2.1), and the Community Multiscale Air Quality (CMAQ) model was applied to investigate the drought impacts on air quality during both drought and normal years in China. Generally, all DR schemes decrease isoprene emissions except for mild drought conditions. The significant decrease and even termination of isoprene emissions are predicted in South China under severe drought conditions. During the drought period, the DR scheme considering both mild and severe drought (SMD) improves the model performance especially in severe drought-hit regions when compared with the Ozone Monitoring Instrument (OMI) averaged formaldehyde vertical column density (HCHO VCD). The results show that most of the DR schemes decrease simulated ozone (O_3) and secondary organic aerosols (SOA) levels. For both O_3 and SOA, noticeable changes are predicted in the Sichuan Basin (5 ppb and 4 μg m^{-3} for O_3 and SOA, respectively). This investigation is the first modeling study to investigate the impacts of isoprene drought response on air quality in China.

Plain Language Summary In the last 50 years, drought has become more severe, prolonged, and frequent in China, which is expected to affect air quality by changing Biogenic volatile organic compound (BVOC) emissions. The BVOCs are regarded as the significant precursor of secondary pollutants such as O_3 and secondary organic aerosols (SOA), and thus play an important role in the air quality. This is the first modeling study to evaluate drought impacts on atmospheric chemistry and air quality in China using different isoprene drought response schemes. The drought scheme considering both mild and severe drought has improved the model performance at severe drought-hit regions when compared with the satellite formaldehyde vertical column density. Most of the drought schemes predict lower isoprene emissions and thus leading to lower O_3 and SOA levels. During the drought year, O_3 and SOA decreases of up to −8% and −30% are simulated for southern China under severe drought conditions.

1. Introduction

Biogenic volatile organic compounds (BVOCs) emitted from terrestrial ecosystems are important precursors to the formation of ozone (O_3) and secondary organic aerosols (SOA) (Fehsenfeld et al., 1992; Xu, Guo, et al., 2015). Among all BVOCs species, isoprene is the most significant precursor due to its large emission quantities and relatively high reactivity with oxidants such as hydroxyl and chlorine radicals (OH and Cl) compared to most anthropogenic VOC species (Dreyfus et al., 2002; Fuentes et al., 2000; Wang & Ruiz, 2017). Biogenic isoprene accounts for approximately 50%–70% of the total BVOC emission globally (Fuentes et al., 2000; Guenther et al., 2006) and about 50% in China (Li et al., 2013; Song et al., 2012).

BVOC emissions are affected by several environmental factors such as temperature, solar radiation, and land cover, which have been relatively well characterized (Arneth et al., 2007; Guenther et al., 2012; Sharkey et al., 1999; Wang, Situ, et al., 2011). Extreme climate conditions such as drought are also expected to affect BVOC emissions due to their impact on plant physiological processes including a reduction in stomatal

10.1029/2020JD033263

Writing – original draft: Peng Wang
Writing – review & editing: Peng Wang, Xuemei Wang, Alex Guenther, Tao Wang

conductance and photosynthesis rates when the soil water content is decreased (Brilli et al., 2007; Centritto et al., 2011; Fortunati et al., 2008; Pegoraro et al., 2004; Rennenberg et al., 2006). The drought response of BVOCs emissions is complicated and depends on the level of stress. Previous laboratory and field studies found that isoprene emissions could remain constant or even increase slightly at the initial phase of a mild drought (Pegoraro et al., 2004; Tingey, 1981; Yuan et al., 2016), but decrease significantly under severe drought conditions (Pegoraro et al., 2004).

Modeling studies have attempted to consider the drought response by using different approaches to investigate the changes in BVOCs and their impacts on air quality. Zhao et al. (2019) applied the Community Multiscale Air Quality (CMAQ) model to describe the drought impacts on SOA in a case study and compared both drought and nondrought periods in the southeast United States. Jiang et al. (2018) applied a soil moisture parameterization to reflect drought response in the Model of Emissions of Gases and Aerosols from Nature (MEGAN) and found that annual isoprene emissions were reduced by 17% globally. Guenther (2001) proposed using a drought index to determine the drought impacts on BVOCs in the global biosphere emissions and interactions system (GLOBEIS) model, a precursor to the MEGAN model, but this method has not been used in previous air quality modeling studies. A comprehensive modeling study is needed to evaluate different drought schemes and their impacts on BVOCs and air quality.

China is impacted by drought every year due to the deficiency of precipitation and higher temperatures (Zhang et al., 2015). More than 140 drought events with durations longer than 3 months were observed during the past 50 years (Wang, Lettenmaier, et al., 2011; Xu, Yang, et al., 2015). In the south and southwest China with high forest coverage, drought has become more frequent and intense, and is expected to continue in the following decades (Dai, 2012; C. -L. Liu et al., 2011; Wang et al., 2014). Therefore, it is of great interest to study the impact of drought on BVOCs emissions and subsequent impacts on air quality in China. Although the MEGAN model version 2.1 (MEGAN 2.1) (Guenther et al., 2012) has been applied to investigate isoprene emissions and their impacts on air quality (Fu et al., 2014; Hu et al., 2017), the drought response was not considered in those previous studies.

The overall objectives of this study are to (1) implement and evaluate different drought response (DR) schemes in the MEGAN model for isoprene predictions in China; (2) investigate the DR impacts on O_3 and SOA formation by using the CMAQ model in the summertime during both drought and non-drought periods. The impacts of the biogenic emissions to O_3 and SOA during drought periods are also discussed. Our study represents to the best of the author's knowledge, the first attempt to investigate the drought response of isoprene emissions and their impacts on air quality in China.

2. Method

2.1. Implementation of the MEGAN Model to Include Drought Effect on Isoprene Emissions

We implement DR in the MEGAN 2.1 because it is widely used to simulate biogenic emissions in China (W. H. Chen et al., 2018; Hu et al., 2017; Y. Liu et al., 2018; Wang, Situ, et al., 2011). In the MEGAN model, drought impacts are estimated through a soil moisture approach (Guenther et al., 2012; Jiang et al., 2018) or by using a drought index (DI) such as the Palmer Drought Severity Index (PDSI) (Yarwood et al., 2002). Previous MEGAN model studies mainly focus on the soil moisture approach. In the present study, the DI approach is also implemented to provide a more comprehensive evaluation of DR. The details of these methods are described in the following sections.

2.1.1. Estimation of Drought Impacts Using the Soil Moisture Approach

In the MEGAN 2.1 model the emission rate (F) of isoprene in each model grid cell (μg h^{-1}) is calculated by Equation 1 (Guenther et al., 2012; Jiang et al., 2018):

$$F = \gamma \times LAI_V \times EF \times A \tag{1}$$

where γ is a lumped activity factor (unitless) that includes the impacts of radiation, leaf temperature, soil moisture (γ_{SM}), leaf age, and CO_2 level on isoprene emission; LAI_v is the leaf area index for the vegetated surface (m^2 of leaf area per m^2 of vegetated surface area); EF is the emission factor of isoprene under standard conditions (μg m^{-2} h^{-1}), and each plant function type (PFT) is assigned a specific EF as described in Guenther et al. (2012); and A is the area of the grid cell (m^2).

The MEGAN 2.1 includes the parameterization of activity factor γ_{SM} as a function of soil moisture and wilting point, as described in Guenther et al. (2012):

$$\begin{aligned} \gamma_{\mathrm{SM,isoprene}} &= 1, && for\ \theta > \theta_1 \\ \gamma_{\mathrm{SM,isoprene}} &= (\theta - \theta_w) / \Delta\theta_1, && for\ \theta_w < \theta < \theta_1, \theta_1 = \Delta\theta_1 + \theta_w \\ \gamma_{\mathrm{SM,isoprene}} &= 0, && for\ \theta < \theta_w \end{aligned} \tag{2}$$

where θ is volumetric soil moisture (m^3 m^{-3}), θ_w is soil moisture at the wilting point, and $\Delta\theta_1$ is an empirical soil moisture amount of 4%–6% ($\Delta\theta_1 = 0.04$ if the wilting point is from Chen & Dudhia, 2001 and $\Delta\theta_1 = 0.06$ for wilting points from the Community Land Model [CLM]). Based on Equation 2, isoprene emissions are terminated when the soil moisture drops below the wilting point. The default values of the wilting point are from Chen and Dudhia (2001) for different soil textures in the offline MEGAN 2.1 used in this study. The soil moisture data used in this study is generated using the Weather Research and Forecasting (WRF) version 4.0.1 with the Noah land surface scheme. The soil moistures in four layers (0–0.1 m, 0.1–0.4 m, 0.4–1 m, 1–2 m) are simulated with long spinup (3 months) and the wilting point is determined based on soil types. Besides the default WRF wilting point data from Chen and Dudhia (2001), the wilting points calculated by the CLM version 4.5 (CLM 4.5), recommended by Jiang et al. (2018), were also applied in this study. For the four soil layers, the $\gamma_{\mathrm{SM,isoprene}}$ is calculated using the identical wilting point data, and the final $\gamma_{\mathrm{SM,isoprene}}$ applied in the MEGAN model ($\gamma_{\mathrm{SM,\ MEGAN}}$) is determined using the following equation:

$$\gamma_{SM,MEGAN} = \sum_{i=1}^{N_{layer}} \sum_{j=1}^{N_{PFT}} \gamma_{SM,i} \times f_{PFT,i,j} \tag{3}$$

where N_{layer} (equals 4) and N_{PFT} (equals 16) are number of soil layers and PFTs; $\gamma_{\mathrm{SM},i}$ is the $\gamma_{SM,isoprene}$ in the ith soil layer calculated by Equation 2; $f_{\mathrm{PFT},i,j}$ is the root zone fraction in the ith soil layer for the jth PFT, and values are from Zeng (2001). This would be further improved if multiplelayer wilting point data were available. The wilting point calculated by CLM 4.5 gives much higher values than the default values throughout China (see Figure S1), which leads to a greater impact of drought on isoprene emissions. In central and southern China regions with higher forest cover, the average wilting point is ~0.2 m^3 m^{-3} in the recommended data set compared to ~0.1 m^3 m^{-3} in the default Chen and Dudhia (2001) data set.

2.1.2. Estimation of Drought Impacts Using the Drought Index Approach

The canopy model (the γ_{CE} function and related subroutines) in the MEGAN 2.1 includes an optional drought parameterization (DIstomata function) on leaf temperature and stomatal conductance as described in Ying, Wang, et al. (2015) Appendix A using PDSI (Dai et al., 2004). In short, the DIstomata function is determined as the following equation.

$$\begin{aligned} \mathrm{DIstomata} &= 1, && \text{for PDSI} > \mathrm{DI_{high}} \\ \mathrm{DIstomata} &= 1 - 0.9 \times (PDSI - DI_{high}) / (DI_{low} - DI_{high}), && \text{for } \mathrm{DI}_{low} < \text{PDSI} \le \mathrm{DI_{low}} \\ \mathrm{DIstomata} &= 0, && \text{for PDSI} \le \mathrm{DI_{low}} \end{aligned} \tag{4}$$

This optional drought parameterization in the MEGAN canopy model was not considered in previous MEGAN studies and was used to calculate the leaf temperature that affected the isoprene emissions in turn. The DIstomata function reflects the stomatal resistance and leads to the higher isoprene emissions (Ying, Wang, et al., 2015), which is only used to describe the isoprene emissions changes under the mild drought condition. Consequently, in this study, $\mathrm{DI_{low}}$ and $\mathrm{DI_{high}}$ equal −2 and −0.5 according to the drought classification (Table S1). Guenther (2001) introduced an implemented drought parameterization associated with water limitations (γ_w) to calculate the isoprene emission under the severe drought. The equations for γ_w are shown in Equation 4:

Table 1
List of Isoprene Emissions Used in This Study

Simulation #	Isoprene emission	Notes
1	BASE	Base case without drought response (DR) scheme
2	MD	Uses PDSI values, ONLY consider the mild drought algorithm ($-2.0 < \text{PDSI} < -0.5$)
3	SMD	Uses PDSI values, consider both mild and severe drought algorithms ($-4.0 \leq \text{PDSI} \leq -0.5$)
4	NSM	Uses wilting point calculated by CLM model
5	SM	Uses wilting point from Chen et al. (2001)

$$
\begin{aligned}
&\gamma_{\text{W,isoprene}} = 1, && \text{for PDSI} > \text{DI}_{\text{min}} \\
&\gamma_{\text{W,isoprene}} = 1 + \left(PDSI - DI_{min}\right) / \left(DI_{min} - DI_{max}\right) && \text{for DI}_{\text{max}} < \text{PDSI} < \text{DI}_{\text{min}} \\
&\gamma_{\text{W,isoprene}} = 0, && \text{for PDSI} < \text{DI}_{\text{max}}
\end{aligned}
\tag{5}
$$

where DI_{min} and DI_{max} are empirical parameters that indicate the PDSI at which emissions begin to decrease and the PDSI at which emission are negligible under extreme drought. In this study, $\text{DI}_{\text{min}} = -2$ and $\text{DI}_{\text{max}} = -4$ are used based on the recommendation in Guenther (2001). Equations 3 and 4 were applied to qualify the drought response in different PDSI ranges. PDSI data sets from National Center for Atmospheric Research (NCAR) website (http://www.cgd.ucar.edu/cas/catalog/climind/pdsi.html) with the horizontal resolution of $2.5° \times 2.5°$ were applied in this study (see Figures S2 and S3).

2.2. Drought Schemes Based on Soil Moisture or Drought Index Approaches

Five sets of isoprene emissions were generated using the MEGAN 2.1 model: (1) only considering the mild drought effects as shown in Equation 3 (MD case), (2) considering both the mild drought (Equation 3) and the severe drought impacts (Equation 4) (SMD case), (3) DR using the CLM 4.5 model calculated wilting point (NSM case), (4) DR using the wilting point from Chen and Dudhia (2001) (SM case), and (5) BASE case. The MD and SMD cases are determined using the drought index approach, and the soil moisture approach is applied in the SM and NSM cases. MD and SMD cases attempt to represent the DR under different drought conditions. The MD case only includes the PDSI parameterization from the MEGAN canopy leaf temperature module (DIstomata function Equation 3), while the SMD also considers the PDSI parameterizations for emission changes due to severe drought (γ_w from Equation 4) conditions (SMD = $\gamma_w \times$ MD). NSM and SM cases aim to evaluate drought impacts driven by different input data (wilting points) through the soil moisture approach. Also, a BASE case without DR schemes is conducted in this study to better understand the role of drought in BVOC emissions. The detailed information for these five simulated cases is summarized in Table 1.

2.3. CMAQ Model and Application

The source-oriented CMAQ model (P. Wang et al., 2018; 2019) with lumped SAPRC-11 (S11L) photochemical mechanism (Carter et al., 2013; Ying, Li, et al., 2015) was applied to study the changes of O_3 and SOA concentrations in China in summer (June, July, and August) 2011 and 2014. The model domain covers all of China and part of East Asia with a horizontal resolution of 36×36 km^2, and the details are described in Wang et al. (2019). Meteorological inputs for the CMAQ model were simulated by the WRF model version 4.0.1, driven by initial and boundary conditions based on the Final (FNL) reanalysis data (ds083.2, https://rda.ucar.edu/datasets/ds083.2/, last access: March, 2021) from the National Centers for Environmental Prediction (NCEP). The detailed WRF model setups were described in Zhang et al. (2012). Anthropogenic emissions in China were obtained from the Multiresolution Emission Inventory for China (MEIC) version 1.0 (He, 2012), and scaled to years 2011 and 2014 based on Ou et al. (2016). The Regional Emission inventory in ASia v2.1 (REAS2) (Kurokawa et al., 2013) was applied to generate emissions for other countries in the model domain. The initial and boundary conditions for the simulation were generated using the CMAQ default profiles which represent clean continental conditions.

Two summers were selected for simulations, one with severe drought and the other being a normal period. In the 2011 summer, the severe and persistent drought occurred in regions with high vegetation cover in southern China, and it was defined as the drought period in this study. In contrast, 2014 was regarded as the normal year (Hou et al., 2015) and was defined as a nondrought period in this study. Figures S2 and S3 show the PDSI in 2011 and 2014, respectively. In 2011, the mild and severe drought occurred in a large part of China from June to August, with severe drought in the middle of Inner Mongolia, north Shaanxi, and most southern China (see Figure S4 and Table S2 for detailed provinces locations and names). In summer 2014, only scattered regions in the North China Plain (NCP) and Yunnan province experienced a severe drought. These two different periods were selected to evaluate DR schemes and drought impacts on air quality.

The model performance (discussed in Section 3.2) is evaluated using the mean fractional bias (MFB), mean fractional error (MFE), mean normal error (MNE), and mean normal bias (MNB), as defined by the following equations:

$$\mathrm{MFB} = \frac{2}{N}\sum_{i=1}^{N}\frac{C_{m,i} - C_{o,i}}{C_{m,i} + C_{o,i}} \tag{6}$$

$$\mathrm{MFE} = \frac{2}{N}\sum_{i=1}^{N}\frac{\left|C_{m,i} - C_{o,i}\right|}{C_{m,i} + C_{o,i}} \tag{7}$$

$$\mathrm{MNB} = \frac{1}{N}\sum_{i=1}^{N}\frac{C_{m,i} - C_{o,i}}{C_{m,i} + C_{o,i}} \tag{8}$$

$$\mathrm{MNE} = \frac{1}{N}\sum_{i=1}^{N}\frac{\left|C_{m,i} - C_{o,i}\right|}{C_{m,i} + C_{o,i}} \tag{9}$$

where I is the number of prediction-observation pairs within the simulation period, and C_m and C_o are model predicted and observed concentrations, respectively.

3. Results and Discussion

3.1. Meteorology Validations

Meteorological factors play a significant role in the predictions of BVOCs and transportation and deposition of air pollutants (Bei et al., 2018; Elminir, 2005; Guenther et al., 2012; Xu et al., 2011). Therefore, the validations of model performance on meteorological conditions are important for the accuracy of air quality predictions. To evaluate the model performance on simulations of meteorological parameters, the observation data were obtained from China National Meteorological Information Center (NMIC, http://data.cma.cn/), including temperature (T2), relative humidity (RH) at 2 m above surface, and wind direction (WD) at 10 m above surface. Statistical parameters of comparison between simulated and observed values including the mean bias (MB), root mean square error (RMSE), index of agreement (IOA), and coefficient of correlation (R) were calculated and are shown in Tables S3 and S4 for 2011 and 2014, respectively. All the statistical formulas and definitions are described in Fan et al. (2013). In general, the WRF model has acceptable performance on the selected indicators and is comparable to other studies using WRF in China (Hu et al., 2015, 2016; Ying et al., 2014; Zhang et al., 2012). For both years, the WRF model predicts slightly lower T2 in the summer time than the observations, indicated by the negative MB values ranging from −0.2 to −0.8. RH is slightly underpredicted in June and July in 2011 and overpredicted in July and August in 2014. In general, the WS is overpredicted in all months, which could enhance the regional transport of air pollution.

3.2. Isoprene Emissions Using Different DR Schemes

Figure 1 shows the simulated average isoprene emissions for the drought period (summer 2011) in China. The total summer isoprene emissions in China are 5.8 Tg (teragram = 10^{12} g), 6.6 Tg, 4.0 Tg, 5.8 Tg, and

10.1029/2020JD033263

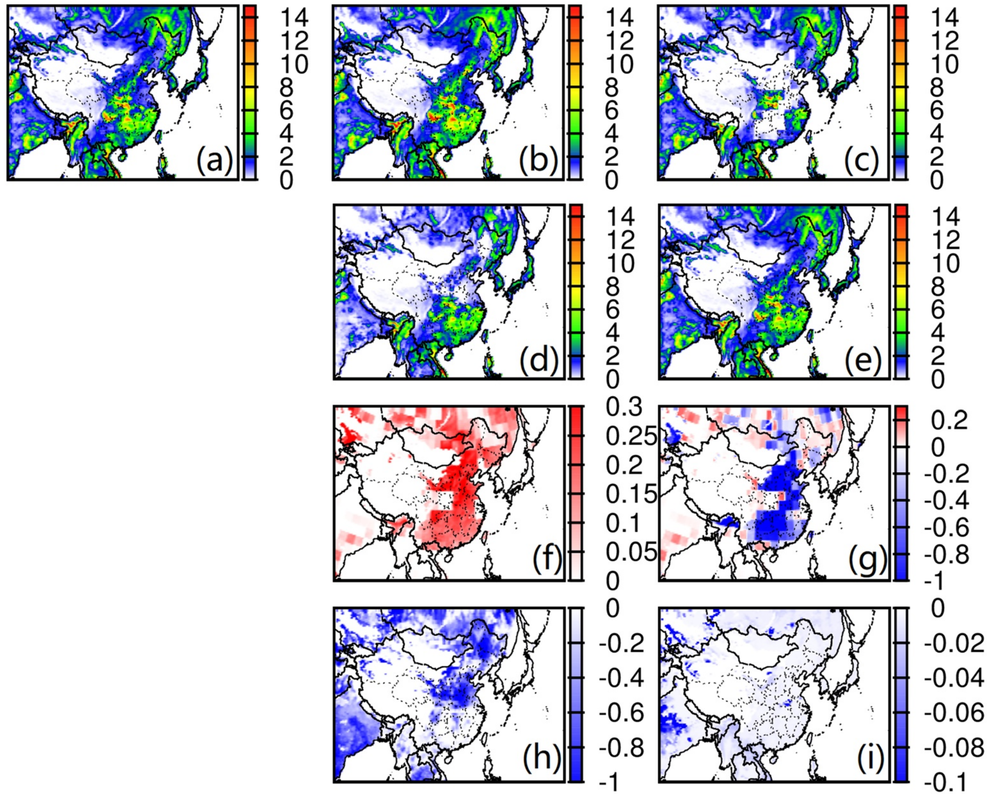

Figure 1. Predicted averaged isoprene emission rate of (a) BASE, (b) MD, (c) SMD, (d) NSM, and (e) SM case, and relative difference (DR case)-BASE/BASE for (f) MD, (g) SMD, (h) NSM, and (i) SM case for a drought episode (summer 2011) in China. Units are moles s^{-1} for (a)–(e). MD, mild drought; SMD, mild and severe drought.

3.5 Tg, for the BASE, MD, NSM, SM, SMD cases, respectively. The MD, NSM, and SM cases have spatial distributions similar to the BASE case with the highest isoprene emissions rate in the Sichuan Basin (SCB), Hunan, and Hubei provinces. The SMD case predicts the lowest emission rates, while the SM case predicts almost the same isoprene emissions as the BASE case (difference <1%) even in drought-hit regions (Hunan, Guangzhou, and Guangxi provinces) of China, indicating that using the default wilting point could not accurately reflect the isoprene drought response (Huang et al., 2015; Jiang et al., 2018; Seco et al., 2015). The MD case estimated the highest emission rates of isoprene, and its increase has the widest spatial distribution through eastern China and in the Beijing-Tianjin-Hebei (BTH), Shanxi province, and southeastern SCB region that suffered from mild droughts, with the enhancement reaching over 30%. During the initial phase of drought, plants conserve water by reducing stomatal conductance, which causes a decrease in evaporative cooling resulting in an increase in leaf temperature. An increase in leaf temperature leads to an increase in isoprene emission (Beckett et al., 2012; Pegoraro et al., 2004). The changes in isoprene emissions are more complex for the SMD case. In severe drought-hit regions, the SMD significantly decreases the isoprene emissions and even terminates the emissions in part of southern China. In mild drought-hit regions such as northeastern China and Henan province, the isoprene emissions increase slightly with the highest increased rate of ∼15%. The decrease in the NSM case mainly occurred in the northern part of China with the highest change of over 80%. In southern China, where there are higher isoprene emissions, the changes caused by the NSM case are relatively small except in the southeastern SCB (with a decrease of ∼40%). Jiang et al. (2018) stated the decrease in the isoprene emissions due to the water stress reached 42% in the drought-hit regions. Zheng et al. (2017) also reported a 54% decrease in the isoprene emissions in the forest region due to the drought impacts, which is highly linked to the photosynthesis process. These results are comparable to this study.

Since no noticeable changes of isoprene emissions are found in the SM case during the drought period (summer 2011), this case is excluded from following discussion (its results are shown in Figures S6, S7,

10.1029/2020JD033263

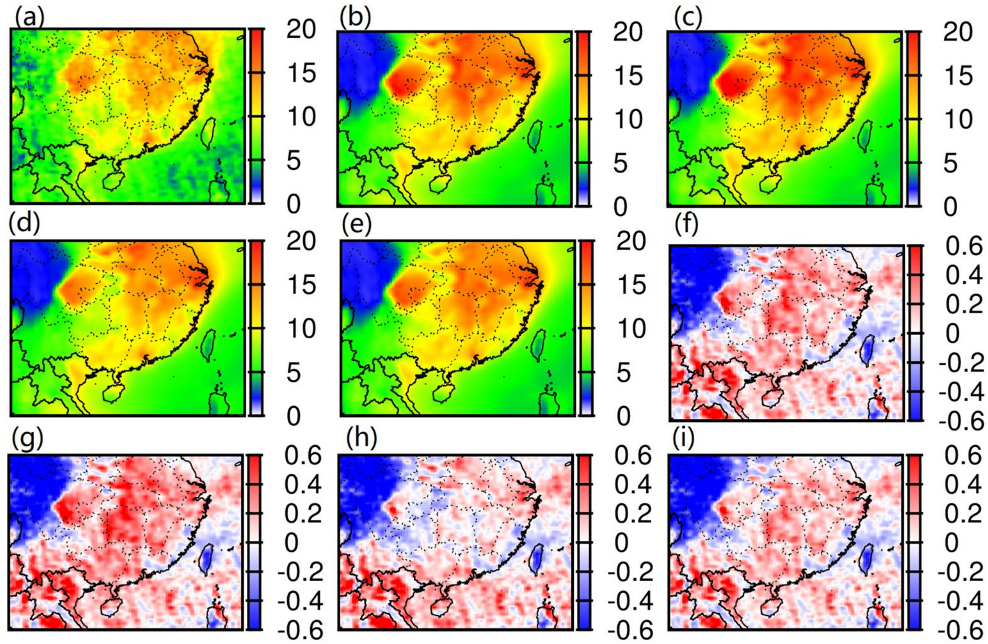

Figure 2. QA4ECV OMI (a) and predicted averaged column density of HCHO for (b) BASE, (c) MD, (d) SMD, and (e) NSM cases ($\times 10^{15}$ molecules cm^{-2}) and relative difference of (Pred.- Obs.)/Obs. Between the observation and (f) BASE, (i) MD, (h) SMD, and (i) NSM cases in summer 2011 in south-eastern China where there are relatively greater drought impacts. MD, mild drought; SMD, mild and severe drought.

and S11) and the model simulation in the normal period (summer 2014) simulations. Figure S5 shows the predicted average isoprene emissions for the normal period in China. As for the drought period, the MD case estimates the highest emission rates of isoprene with the relative increase of up to 30% in northern China followed by the BASE case. In southeastern China with high forest cover, a smaller decrease (<20%) in isoprene emissions is simulated for the SMD and NSM cases in the normal year compared to that in the drought year (up to 100%), which is also reported in Jiang et al. (2018).

3.3. Drought Scheme Evaluations in Drought and Nondrought Periods

To help evaluate different DR schemes, we made use of the column density of formaldehyde (HCHO) measured by the Ozone Monitoring Instrument (OMI) (De Smedt et al., 2018). In the summertime, isoprene is the dominant source of HCHO in vegetated regions because HCHO is a key product of isoprene oxidation reactions, and comparisons between predicted and observed HCHO concentrations are an effective way to evaluate the accuracy of isoprene emissions (Palmer et al., 2003; Zheng et al., 2017). In this study, the 0.25° × 0.25° gridded monthly average HCHO vertical column density (VCD) data were taken from EU FP7-project Quality Assurance for Essential Climate Variables (QA4ECV, http://www.qa4ecv.eu/ecv/hcho-p/data last access: August 2020). Figure 2 (contains southeastern China), Figures S6 and S8 show the comparison results between the OMI satellite data and all predicted cases in drought and normal periods in China, respectively. In the study, the CMAQ HCHO VCD retrieval approach is based on Wang et al. (2017) with the consideration of the satellite passing time, cloud cover and other factors. The sum of qualified predicted HCHO from all vertical layers within the troposphere in the CMAQ model (17 layers, total ~10 km with the first layer ~35 m above the surface) is calculated to match the monthly averaged HCHO VCD data.

In general, the slightly higher HCHO VCD in the normal period is found in southern China where there is high forest cover (Figure S8) compared to that in the drought period from OMI satellite data, partially indicating the drought impacts in this region. For instance, in Hunan province (average forest cover >50% and PDSI <−4 in summer 2011), a decrease of HCHO VCD (up to 30%) is observed and attributed to the occurrence of drought. The similar results are also found in the predicted HCHO VCD. Compared to the drought period, the higher HCHO VCD are simulated in the Hunan, Hubei, and Jiangxi provinces. Other factors such as the meteorological condition (including the slight temperature) and uncertainties in the anthropogenic emission inventory may also contribute to the higher HCHO VCD in the nondrought period. For both drought and normal periods, all predicted cases including the base case could reproduce the spatial distribution of the HCHO VCD satellite data. Overestimations of HCHO VCD are generally found in southern China such as Guangxi and Hunan provinces for all predicted cases in both periods. The under-estimations in the NCP such as Shandong province during the drought period is mainly due to missing HCHO anthropogenic sources.

Tables S5 and S6 show MFB and MFE for all predicted cases in drought and normal periods, respectively. Grids with forest cover larger than 50% in southern China (see Figure S9) are selected to represent HCHO dominated by biogenic sources, and a cutoff HCHO VCD value of 5×10^{15} molecules cm^{-2} is applied to exclude the influence of extremely low concentrations and impacts from background HCHO (Boeke et al., 2011; De Smedt et al., 2018). Also, we omitted data from June to exclude the impacts of the higher biomass burning sector at that time (J. Chen et al., 2017).

Figure S10 illustrates scatter plots that compare predicted and observed HCHO VCD in the same selected grids in the drought period (summer 2011). The predicted and observed HCHO VCD are within a factor of 2, and the similar model performance is also reported in Zheng et al. (2017). All simulations have similar correlation coefficients, ranging from 0.610 (MD) to 0.651 (NSM). The positive MFB values indicate that all the predicted cases have slightly over-estimated the HCHO VCD in the drought period (Table S5). Based on these statistical results, SMD (overall MFB = −0.018, MFE = 0.198, $R = 0.624$) and NSM cases (overall MFB = 0.066, MFE = 0.216, $R = 0.651$) improve the model performance to a certain degree. We also further evaluated the model performance in drought-hit regions (PDSI ≤ -0.5). The NSM case has a slightly better model performance under the mild drought condition ($-2.0 \leq$ PDSI ≤ -0.5) with overall MFB = 0.054, MFE = 0.222, and $R = 0.619$ (see Figure 3 and Table 2). Simultaneously, under the severe drought (PDSI < -2.0), the SMD case has the best model performance with overall MFB = −0.019, MFE = 0.178, and $R = 0.623$. Especially in August when stronger drought occurred, SMD has a prominently improved model performance, with MFB = −0.001 and MFE = 0.170 compared to 0.157 and 0.223 in the BASE case. The SMD case predicted the lower HCHO VCD under severe drought while slightly overestimating under mild drought. We suggest that SMD could be used in the MEGAN model during the drought period, especially in severe drought-hit regions.

In the normal period (summer 2014), surface measurements of maximum daily averaged 8 h (MDA8) O_3 and hourly fine particulate matter ($PM_{2.5}$) were used to evaluate the DR schemes as well as the OMI HCHO VCD. These surface measurements were operated by the Ministry of Ecology and Environment (MEE) of China since 2013 (no data are available in 2011) and a total of 269 sites with validated data throughout China were included in this study (see Figure S12). Unlike the drought period, the BASE case slightly under-estimated the HCHO VCD in high forest cover regions (See Table S6 and Figure S13) in the normal period, which may partially explain the missing drought scheme being one of the factors causing the isoprene overestimation. For both drought and normal periods, the NSM case predicts the lower HCHO VCD compared to that of the BASE case. Previous studies showed the overestimation of isoprene emissions in the default MEGAN model (BASE case) at various regions (Hu et al., 2017; Kota et al., 2015; Wang et al., 2017). The NSM scheme may help to alleviate the overestimation problem due to the lower predicted isoprene emission rates.

Considering the surface measurements comparison (Table S7), the model performances are all within the criteria [EPA, 2005; 2007] (MNB $\leq \pm 0.15$, MNE ≤ 0.3, and MFB $\leq \pm 0.6$, MFE ≤ 0.75 for MDA8 O_3 and $PM_{2.5}$, respectively). All these four predicted cases have slightly overestimated the MDA8 O_3 upto 2.4 ppb (MD case), while underestimating $PM_{2.5}$. For MDA8 O_3, the NSM has a slightly better model performance (MNB = 0.06 and MNE = 0.25) and similar model performances are found in $PM_{2.5}$ for all predicted cases. In summary, no noticeable changes are discovered between the BASE and drought schemes in the normal episode according to differences of the O_3 and $PM_{2.5}$.

In this study, we comprehensively evaluate the drought schemes through comparisons of satellite HCHO VCD. However, uncertainties exist in the evaluation process from multiple sources. First, the HCHO VCD data set may contain retrieval algorithm errors such as errors of slant column retrieval and the air mass

10.1029/2020JD033263

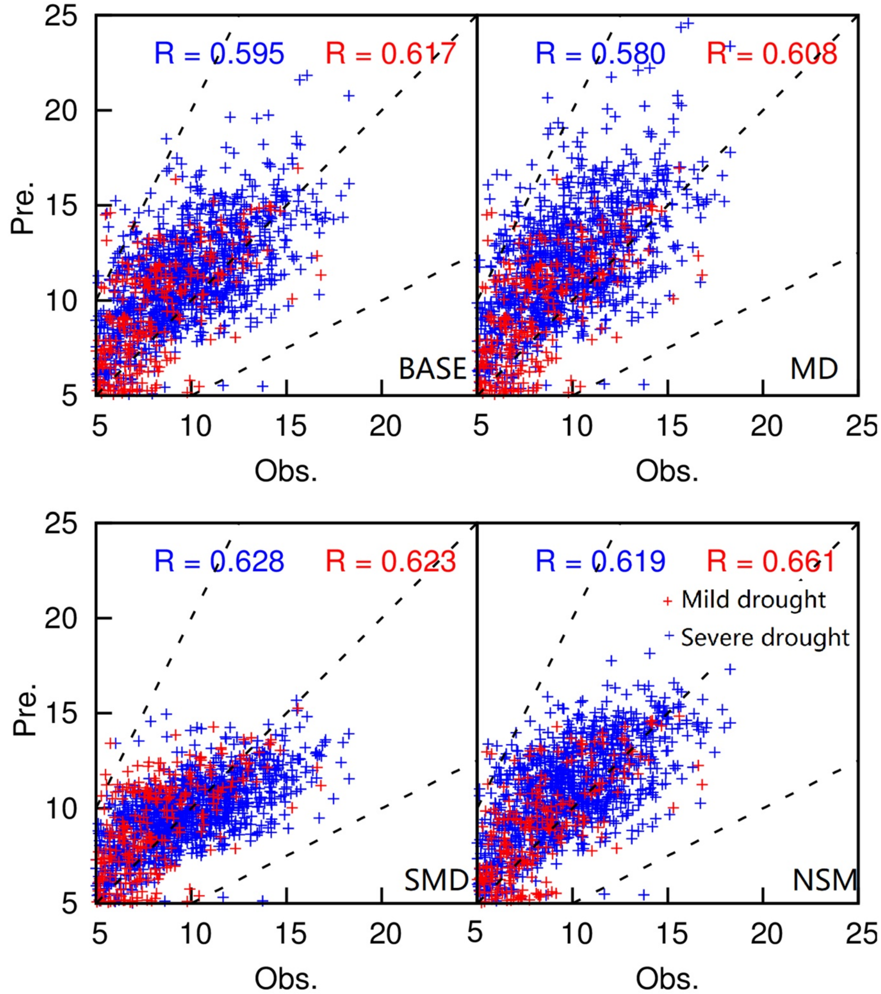

Figure 3. CMAQ predicted HCHO VCD versus OMI monthly HCHO columns for the drought period (summer 2011). The dash lines are 1:1, 1:2 and 2:1 ratio. Grids with drought and forest cover larger than 50% and HCHO VCD concentration higher than 5×10^{15} molecules cm^{-2} are selected.

Table 2
Mean Fractional Bias (MFB) and Mean Fractional Error (MFE) of Column Formaldehyde (HCHO) for Summer 2011 in China.

		MFB			MFE		
Simulations	Drought condition	July	August	All	July	August	All
BASE	MD*	0.184	0.041	0.106	0.258	0.228	0.242
	SD*	0.096	0.157	0.127	0.222	0.223	0.222
MD	MD	0.226	0.091	0.152	0.253	0.262	0.244
	SD	0.148	0.216	0.182	0.253	0.261	0.257
SMD	MD	0.155	0.002	0.071	0.245	0.211	0.226
	SD	−0.019	−0.001	−0.01	0.185	0.17	0.178
NSM	MD	0.091	−0.056	0.054	0.198	0.241	0.222
	SD	0.065	0.125	0.095	0.202	0.204	0.204

Grids with drought condition and forest cover larger than 50% and HCHO VCD concentration higher than 5×10^{15} molecules cm^{-2} are selected. * MD stands for the mild drought and SD stands for the severe drought.

10.1029/2020JD033263

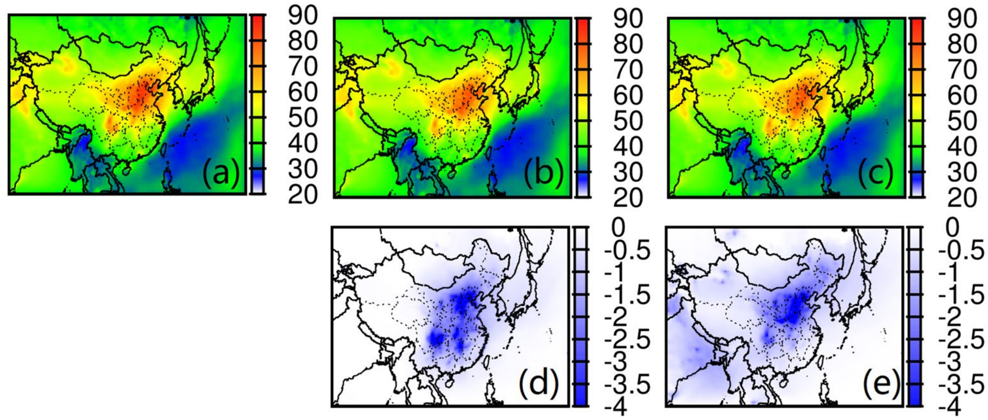

Figure 4. MDA8 O_3 mixing ratio for (a) BASE, (b) SMD, and (c) NSM cases and the absolute difference between the BASE case and (d) MD, and (e) SMD cases for drought period (summer 2011) in China. The absolute difference is (DR case-Base case). Units are ppb. MD, mild drought; SMD, mild and severe drought.

factor uncertainty associated with clouds, aerosol and profile shape impacts (De Smedt et al., 2018). Second, the anthropogenic VOCs and other BVOCs such as monoterpenes could also introduce uncertainties in the evaluation process since they may form HCHO through oxidation reactions (Han et al., 2013). Third, the WRF model has overestimated the wind speed, which may affect the regional transport and distributions of the HCHO concentrations in the air quality model. Other WRF model predicted meteorology parameters such as the planetary boundary layer height are different under drought conditions (Zheng et al., 2017), which may also introduce uncertainties in the study.

3.4. MDA O_3 and SOA Changes due to Different DR Schemes

Figures 4, S14, and Figure 5, S16 show the predicted MDA8 O_3 mixing ratios and SOA concentrations of all predicted cases and their absolute differences caused by the different DR schemes in the drought period, respectively. In the SCB that suffered drought, higher levels of these secondary pollutants (O_3 and SOA) are found, with the peak values up to 75 ppb for O_3 and 18 $\mu g\ m^{-3}$ for SOA. In general, the SMD and NSM cases predict lower levels of these secondary pollutants due to declined isoprene emissions while the MD case increases their concentrations. The most significant decreases for both O_3 and SOA are found in the SMD case. In drought-hit regions in southern China (e.g., the SCB, Hunan, and Guizhou provinces), the SMD induces a decrease of more than 4 ppb in MDA8 O_3. Previous study also found the lower isoprene emissions decreased the O_3 concentration (~3 ppb) (Jiang et al., 2018), which is close to this study. Similar

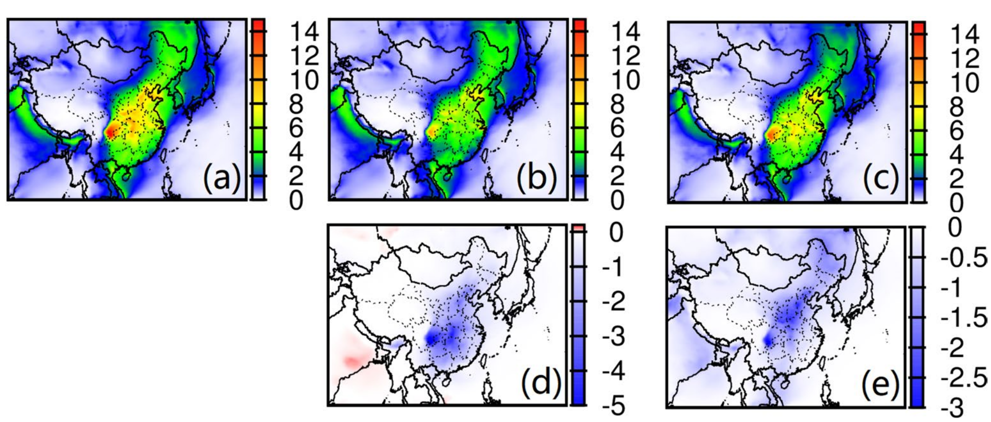

Figure 5. Predicted average SOA concentrations for (a) BASE, (b) SMD, and (c) NSM cases and the absolute difference (DR case-Base case) between the BASE case and (d) SMD, and (e) NSM cases for drought period (summer 2011) in China. Units are $\mu g\ m^{-3}$. MD, mild drought; SOA, secondary organic aerosols; SMD, mild and severe drought.

10.1029/2020JD033263

to O_3, significant SOA reductions (up to ∼3 μg m^{-3}) are also observed in these regions in the SMD case. In addition, reductions of these secondary pollutants are also found in the NCP, especially in the NSM case, which is mainly due to lower isoprene emissions and the regional transport under impacts of southerly wind. For all predicted cases, the SOA is a major contributor to total OA (fSOA = SOA/total OA) in summer (as shown in Figure S17), which is consistent with a previous study (Hu et al., 2017). For the NSM and SMD cases, the decreases in fSOA cover a large portion of southern China in which more OA is generated from the primary sources due to the decrease in isoprene emissions. In the normal period, fewer changes of O_3 and SOA are found in these DR cases except for the NSM (Figure S17 and S18). More prominent decreases in O_3 (more than 4 ppb) and SOA (more than 3 μg m^{-3}) were observed for the NSM case, covering a large area in China for the normal period. This indicates that the NSM case has important impacts on air quality even during the normal period. Long-term soil moisture observations are also needed to better constrain the WRF-predicted soil moisture in the NSM scheme.

In both drought and normal periods, DR schemes introduced important changes of secondary pollutants in the SCB, one of the most polluted regions in China (Qiao et al., 2015). More comprehensive strategies with the consideration of extreme meteorological conditions such as drought are required to improve air quality in this region.

4. Summary

This study has investigated the drought impacts from different DR schemes during both drought and non-drought years. More important impacts of DR schemes on isoprene emissions are found in the drought period. In general, most DR schemes predict lower isoprene emissions in southern China where severe drought occurs and leads to lower O_3 and SOA levels. The key findings include:

(1) Significant decreases or even terminations of isoprene emissions are found in severe drought-hit regions. However, rising isoprene emissions (upto 30%) occur under mild drought conditions
(2) The drought scheme for both mild and severe drought (SMD) improves the model performance in severe drought-hit regions, with the MFB = −0.01 and MFE = 0.18
(3) In drought-hit regions, reductions of O_3 and SOA reach up to 8% and 30%, respectively during the drought year

This study revealed that model simulations of drought impacts are highly sensitive to the input data. More work should be conducted addressing drought response since persistent drought now occurs more frequently in China and elsewhere and its impacts may increase in the coming decades. A higher resolution drought index, more accurate wilting point, and observed soil moisture data are required. Also, since uncertainties are reported in the satellite data used in this study, introduced by multiple factors such as the anthropogenic emissions and meteorology parameters. The long-term observation data of isoprene emissions and concentrations, covering periods including both drought and nondrought years, are urgently needed to evaluate and improve the current DR scheme algorithms. Moreover, a locally parameterized MEGAN model is required to better understand the BVOCs emissions in China. This study demonstrates the potential drought impacts on air quality in China and indicates that more efforts should be made to better understand, evaluate, and simulate the controlling processes.

Conflict of Interest

The authors declare that they have no conflict of interest.

Data Availability Statement

The data archiving is at https://zenodo.org/record/4638265#.YF05B-gzZEY.

10.1029/2020JD033263

Acknowledgments

This work was supported by a grant from the Research Grants Council of the Hong Kong Special Administrative Region, China (Project No. T24/504/17 and A-PolyU502/16). A. Guenther was supported by National Science Foundation (NSF) Atmospheric Chemistry program award AGS1643042.

References

Arneth, A., Niinemets, Ü., Pressley, S., Bäck, J., Hari, P., Karl, T., et al. (2007). Process-based estimates of terrestrial ecosystem isoprene emissions: Incorporating the effects of a direct CO_2-isoprene interaction. *Atmospheric Chemistry and Physics*, *7*, 31–53. https://doi.org/10.5194/acp-7-31-2007

Beckett, M., Loreto, F., Velikova, V., Brunetti, C., Di Ferdinando, M., Tattini, M., et al. (2012). Photosynthetic limitations and volatile and non-volatile isoprenoids in the poikilochlorophyllous resurrection plant Xerophyta humilis during dehydration and rehydration. *Plant, Cell and Environment*, *35*, 2061–2074. https://doi.org/10.1111/j.1365-3040.2012.02536.x

Bei, N., Zhao, L., Wu, J., Li, X., Feng, T., & Li, G. (2018). Impacts of sea-land and mountain-valley circulations on the air pollution in Beijing-Tianjin-Hebei (BTH): A case study. *Environmental Pollution*, *234*, 429–438. https://doi.org/10.1016/j.envpol.2017.11.066

Boeke, N. L., Marshall, J. D., Alvarez, S., Chance, K. V., Fried, A., Kurosu, T. P., et al. (2011). Formaldehyde columns from the Ozone Monitoring Instrument: Urban versus background levels and evaluation using aircraft data and a global model. *Journal of Geophysical Research*, *116*(D5). https://doi.org/10.1029/2010jd014870

Brilli, F., Barta, C., Fortunati, A., Lerdau, M., Loreto, F., & Centritto, M. (2007). Response of isoprene emission and carbon metabolism to drought in white poplar (Populus alba) saplings. *New Phytologist*, *175*, 244–254. https://doi.org/10.1111/j.1469-8137.2007.02094.x

Carter, W. P. L., & Heo, G. (2013). Development of revised SAPRC aromatics mechanisms. *Atmospheric Environment*, *77*, 404–414. https://doi.org/10.1016/j.atmosenv.2013.05.021

Centritto, M., Brilli, F., Fodale, R., & Loreto, F. (2011). Different sensitivity of isoprene emission, respiration and photosynthesis to high growth temperature coupled with drought stress in black poplar (Populus nigra) saplings. *Tree Physiology*, *31*, 275–286. https://doi.org/10.1093/treephys/tpq112

Chen, F., & Dudhia, J. (2001). Coupling an advanced land surface-hydrology model with the Penn state-NCAR MM5 modeling system. Part I: Model implementation and sensitivity. *Monthly Weather Review*, *129*, 569–585. https://doi.org/10.1175/1520-0493(2001)129<0569:caalsh>2.0.co;2

Chen, J., Li, C., Ristovski, Z., Milic, A., Gu, Y., Islam, M. S., et al. (2017). A review of biomass burning: Emissions and impacts on air quality, health and climate in China. *The Science of the Total Environment*, *579*, 1000–1034. https://doi.org/10.1016/j.scitotenv.2016.11.025

Chen, W. H., Guenther, A. B., Wang, X. M., Chen, Y. H., Gu, D. S., Chang, M., et al. (2018). Regional to global biogenic isoprene emission responses to changes in vegetation from 2000 to 2015. *Journal of Geophysical Research: Atmospheres*, *123*, 3757–3771. https://doi.org/10.1002/2017JD027934

Dai, A. (2012). Increasing drought under global warming in observations and models. *Nature Climate Change*, *3*, 52–58. https://doi.org/10.1038/nclimate1633

Dai, A., Trenberth, K. E., & Qian, T. (2004). A global dataset of palmer drought severity index for 1870-2002: Relationship with soil moisture and effects of surface warming. *Journal of Hydrometeorology*, *5*, 1117–1130. https://doi.org/10.1175/jhm-386.1

De Smedt, I., Theys, N., Yu, H., Danckaert, T., Lerot, C., Compernolle, S., et al. (2018). Algorithm theoretical baseline for formaldehyde retrievals from S5P TROPOMI and from the QA4ECV project. *Atmospheric Measurement Techniques*, *11*, 2395–2426. https://doi.org/10.5194/amt-11-2395-2018

Dreyfus, G. B., Schade, G. W., & Goldstein, A. H. (2002). Observational constraints on the contribution of isoprene oxidation to ozone production on the western slope of the Sierra Nevada, California. *Journal of Geophysical Research*, *107*(D19), 4365. https://doi.org/10.1029/2001jd001490

Elminir, H. K. (2005). Dependence of urban air pollutants on meteorology. *The Science of the Total Environment*, *350*, 225–237. https://doi.org/10.1016/j.scitotenv.2005.01.043

EPA. (2005), *Guidance on the use of models and other analyses in attainment demonstrations for the 8-hour ozone NAAQS Report*. US Environmental Protection Agency.

EPA. (2007). *Guidance on the use of models and other analyses for demonstrating attainment of air quality goals for ozone, PM2. 5, and regional haze*. US Environmental Protection Agency, Office of Air Quality Planning and Standards.

Fan, Q., Liu, Y., Wang, X., Fan, S., Chan, P. W., Lan, J., & Feng, Y. (2013). Effect of different meteorological fields on the regional air quality modelling over Pearl River Delta, China. *International Journal of Environment and Pollution*, *53*, 3–23. https://doi.org/10.1504/ijep.2013.058816

Fehsenfeld, F., Calvert, J., Fall, R., Goldan, P., Guenther, A. B., Hewitt, C. N., et al. (1992). Emissions of volatile organic compounds from vegetation and the implications for atmospheric chemistry. *Global Biogeochemical Cycles*, *6*, 389–430. https://doi.org/10.1029/92gb02125

Fortunati, A., Barta, C., Brilli, F., Centritto, M., Zimmer, I., Schnitzler, J. -P., & Loreto, F. (2008). Isoprene emission is not temperature-dependent during and after severe drought-stress: A physiological and biochemical analysis. *Plant Journal*, *55*, 687–697. https://doi.org/10.1111/j.1365-313X.2008.03538.x

Fu, Y., Liao, H. (2014), Impacts of land use and land cover changes on biogenic emissions of volatile organic compounds in China from the late 1980s to the mid-2000s: Implications for tropospheric ozone and secondary organic aerosol. *Tellus B: Chemical and Physical Meteorology*, *66*, 24987. https://doi.org/10.3402/tellusb.v66.24987

Fuentes, J. D., Gu, L., Lerdau, M., Atkinson, R., Baldocchi, D., Bottenheim, J. W., et al. (2000). Biogenic hydrocarbons in the atmospheric boundary layer: A review. *Bulletin of the American Meteorological Society*, *81*, 1537–1575. https://doi.org/10.1175/1520-0477(2000)081<1537:bhitab>2.3.co;2

Guenther, A. (2001). *Review of the effects of drought and high temperature on biogenic emissions and future research efforts in Texas* (p. 16). National Center for Atmospheric Research, Texas natural Resource Conservation Commission.

Guenther, A. B., Jiang, X., Heald, C. L., Sakulyanontvittaya, T., Duhl, T., Emmons, L. K., & Wang, X. (2012). The model of emissions of gases and aerosols from nature version 2.1 (MEGAN2.1): An extended and updated framework for modeling biogenic emissions. *Geoscientific Model Development*, *5*, 1471–1492. https://doi.org/10.5194/gmd-5-1471-2012

Guenther, A. B., Karl, T., Harley, P., Wiedinmyer, C., Palmer, P. I., & Geron, C. (2006). Estimates of global terrestrial isoprene emissions using MEGAN (model of emissions of gases and aerosols from nature). *Atmospheric Chemistry and Physics*, *6*, 3181–3210. https://doi.org/10.5194/acp-6-3181-2006

Han, K. M., Park, R. S., Kim, H. K., Woo, J. H., Kim, J., & Song, C. H. (2013). Uncertainty in biogenic isoprene emissions and its impacts on tropospheric chemistry in East Asia. *The Science of the Total Environment*, *463–464*, 754–771. https://doi.org/10.1016/j.scitotenv.2013.06.003

He, K. (2012). Multi-resolution emission inventory for China (MEIC): Model framework and 1990-2010 anthropogenic emissions. *Paper presented at AGU fall meeting abstracts*. Retrieved from http://www.meicmodel.org/

Hou, W., Chen, Y., Li, Y., Wang, Y., Wang, Z., Zhu, X., et al. (2015). Climatic characteristics over China in 2014. *Meteorological Monthly*, *41*, 480–488.

Hu, J., Chen, J., Ying, Q., & Zhang, H. (2016). One-year simulation of ozone and particulate matter in China using WRF/CMAQ modeling system. *Atmospheric Chemistry and Physics*, *16*. https://doi.org/10.5194/acp-16-10333-2016

Hu, J., Wang, P., Ying, Q., Zhang, H., Chen, J., Ge, X., et al. (2017). Modeling biogenic and anthropogenic secondary organic aerosol in China. *Atmospheric Chemistry and Physics*, *17*, 77–92. https://doi.org/10.5194/acp-17-77-2017

Hu, J., Wu, L., Zheng, B., Zhang, Q., He, K., Chang, Q., et al. (2015). Source contributions and regional transport of primary particulate matter in China. *Environmental Pollution*, *207*, 31–42. https://doi.org/10.1016/j.envpol.2015.08.037

Huang, L., McGaughey, G., McDonald-Buller, E., Kimura, Y., & Allen, D. T. (2015). Quantifying regional, seasonal and interannual contributions of environmental factors on isoprene and monoterpene emissions estimates over eastern Texas. *Atmospheric Environment*, *106*, 120–128. https://doi.org/10.1016/j.atmosenv.2015.01.072

Jiang, X., Guenther, A., Potosnak, M., Geron, C., Seco, R., Karl, T., et al. (2018). Isoprene emission response to drought and the impact on global atmospheric chemistry. *Atmospheric Environment*, *183*, 69–83. https://doi.org/10.1016/j.atmosenv.2018.01.026

Kota, S. H., Schade, G., Estes, M., Boyer, D., & Ying, Q. (2015). Evaluation of MEGAN predicted biogenic isoprene emissions at urban locations in Southeast Texas. *Atmospheric Environment*, *110*, 54–64. https://doi.org/10.1016/j.atmosenv.2015.03.027

Kurokawa, J., Ohara, T., Morikawa, T., Hanayama, S., Janssens-Maenhout, G., Fukui, T., et al. (2013). Emissions of air pollutants and greenhouse gases over Asian regions during 2000-2008: Regional Emission inventory in Asia (REAS) version 2. *Atmospheric Chemistry and Physics*, *13*, 11019–11058. https://doi.org/10.5194/acp-13-11019-2013

Li, L. Y., Chen, Y., & Xie, S. D. (2013). Spatio-temporal variation of biogenic volatile organic compounds emissions in China. *Environmental Pollution*, *182*, 157–168. https://doi.org/10.1016/j.envpol.2013.06.042

Liu, C.-L., Zhang, Q., Singh, V. P., & Cui, Y. (2011). Copula-based evaluations of drought variations in Guangdong, South China. *Natural Hazards*, *59*(3), 1533–1546. https://doi.org/10.1007/s11069-011-9850-4

Liu, Y., Li, L., An, J., Huang, L., Yan, R., Huang, C., et al. (2018). Estimation of biogenic VOC emissions and its impact on ozone formation over the Yangtze River Delta region, China. *Atmospheric Environment*, *186*, 113–128. https://doi.org/10.1016/j.atmosenv.2018.05.027

Ou, J., Yuan, Z., Zheng, J., Huang, Z., Shao, M., Li, Z., et al. (2016). Ambient ozone control in a photochemically active region: Short-term despiking or long-term attainment? *Environmental Science & Technology*, *50*, 5720–5728. https://doi.org/10.1021/acs.est.6b00345

Palmer, P. I., Jacob, D. J., Fiore, A. M., Martin, R. V., Chance, K., & Kurosu, T. P. (2003). Mapping isoprene emissions over North America using formaldehyde column observations from space. *Journal of Geophysical Research*, *108*(D6). https://doi.org/10.1029/2002jd002153

Pegoraro, E., Rey, A., Greenberg, J., Harley, P., Grace, J., Malhi, Y., & Guenther, A. (2004). Effect of drought on isoprene emission rates from leaves of Quercus virginiana Mill. *Atmospheric Environment*, *38*, 6149–6156. https://doi.org/10.1016/j.atmosenv.2004.07.028

Qiao, X., Jaffe, D., Tang, Y., Bresnahan, M., & Song, J. (2015). Evaluation of air quality in Chengdu, Sichuan Basin, China: Are China's air quality standards sufficient yet? *Environmental Monitoring and Assessment*, *187*, 250. https://doi.org/10.1007/s10661-015-4500-z

Rennenberg, H., Loreto, F., Polle, A., Brilli, F., Fares, S., Beniwal, R. S., & Gessler, A. (2006). Physiological responses of forest trees to heat and drought. *Plant Biology*, *8*, 556–571. https://doi.org/10.1055/s-2006-924084

Seco, R., Karl, T., Guenther, A., Hosman, K. P., Pallardy, S. G., Gu, L., et al. (2015). Ecosystem-scale volatile organic compound fluxes during an extreme drought in a broadleaf temperate forest of the Missouri Ozarks (central USA). *Global Change Biology*, *21*, 3657–3674. https://doi.org/10.1111/gcb.12980

Sharkey, T. D., Singsaas, E. L., Lerdau, M. T., & Geron, C. D. (1999). Weather effects on isoprene emission capacity and applications in emissions algorithms. *Ecological Applications*, *9*, 1132–1137. https://doi.org/10.2307/264138310.1890/1051-0761(1999)009[1132:weoiec]2.0.co;2

Song, Y., Zhang, Y., Wang, Q., & An, J. (2012). Estimation of biogenic VOCs emissions in Eastern China based on remote sensing data. *Acta Scientiae Circumstantiae*, *32*, 2216–2227.

Tingey, D. (1981). *The effect of environmental factors on the emission of biogenic hydrocarbons from live oak and slash pine [Pinus elliottii, Quercus virginiana, USA]* (pp. 53–79).

Wang, A., Lettenmaier, D. P., & Sheffield, J. (2011a). Soil moisture drought in China, 1950-2006. *Journal of Climate*, *24*, 3257–3271. https://doi.org/10.1175/2011jcli3733.1

Wang, D. S., & Ruiz, L. H. (2017). Secondary organic aerosol from chlorine-initiated oxidation of isoprene. *Atmospheric Chemistry and Physics*, *17*, 13491–13508. https://doi.org/10.5194/acp-17-13491-2017

Wang, L., & Chen, W. (2014). A CMIP5 multimodel projection of future temperature, precipitation, and climatological drought in China. *International Journal of Climatology*, *34*, 2059–2078. https://doi.org/10.1002/joc.3822

Wang, P., Chen, Y., Hu, J., Zhang, H., & Ying, Q. (2018). Attribution of Tropospheric Ozone to NOx and VOC Emissions: Considering Ozone Formation in the Transition Regime. *Environ. Sci. Technol.*, *53*(3), 1404–1412. https://doi.org/10.1021/acs.est.8b05981

Wang, P., Chen, Y., Hu, J., Zhang, H., & Ying, Q. (2019). Source apportionment of summertime ozone in China using a source-oriented chemical transport model. *Atmospheric Environment*, *211*, 79–90. https://doi.org/10.1016/j.atmosenv.2019.05.006

Wang, P., Schade, G., Estes, M., & Ying, Q. (2017). Improved MEGAN predictions of biogenic isoprene in the contiguous United States. *Atmospheric Environment*, *148*, 337–351. https://doi.org/10.1016/j.atmosenv.2016.11.006

Wang, X., Situ, S., Guenther, A., Chen, F., Wu, Z., Xia, B., & Wang, T. (2011b). Spatiotemporal variability of biogenic terpenoid emissions in Pearl River Delta, China, with high-resolution land-cover and meteorological data. *Tellus B: Chemical and Physical Meteorology*, *63*, 241–254. https://doi.org/10.1111/j.1600-0889.2010.00523.x

Xu, K., Yang, D., Yang, H., Li, Z., Qin, Y., & Shen, Y. (2015a). Spatio-temporal variation of drought in China during 1961-2012: A climatic perspective. *Journal of Hydrology*, *526*, 253–264. https://doi.org/10.1016/j.jhydrol.2014.09.047

Xu, L., Guo, H., Boyd, C. M., Klein, M., Bougiatioti, A., Cerully, K. M., et al. (2015b). Effects of anthropogenic emissions on aerosol formation from isoprene and monoterpenes in the southeastern United States. *Proceedings of the National Academy of Sciences of the United States of America*, *112*, 37–42. https://doi.org/10.1073/pnas.1417609112

Xu, W. Y., Zhao, C. S., Ran, L., Deng, Z. Z., Liu, P. F., Ma, N., et al. (2011). Characteristics of pollutants and their correlation to meteorological conditions at a suburban site in the North China Plain. *Atmospheric Chemistry and Physics*, *11*, 4353–4369. https://doi.org/10.5194/acp-11-4353-2011

Yarwood, G., Wilson, G., Shepard, S., & Guenther, A. (2002). *User's guide to the global biosphere emissions and interactions system(GloBEIS) version* (3, p. 773). ENVIRON International Corporation.

Ying, Q., Li, J., & Kota, S. H. (2015a). Significant contributions of isoprene to summertime secondary organic aerosol in eastern United States. *Environmental Science & Technology*, *49*(13), 7834–7842. https://doi.org/10.1021/acs.est.5b02514

10.1029/2020JD033263

Ying, Q., Wang, P., Gao, H., & Schade, G. (2015b). *Improving modeled biogenic isoprene emissions under drought conditions and evaluating their impact on ozone formation* (pp. 1–108). Retrieved from http://aqrp.ceer.utexas.edu/projectinfoFY14_15%5C14-030%5C14-030%20Final%20Report.pdf

Ying, Q., Wu, L., & Zhang, H. (2014). Local and inter-regional contributions to PM2.5 nitrate and sulfate in China. *Atmospheric Environment*, *94*, 582–592. https://doi.org/10.1016/j.atmosenv.2014.05.078

Yuan, X., Calatayud, V., Gao, F., Fares, S., Paoletti, E., Tian, Y., & Feng, Z. (2016). Interaction of drought and ozone exposure on isoprene emission from extensively cultivated poplar. *Plant, Cell and Environment*, *39*, 2276–2287. https://doi.org/10.1111/pce.12798

Zeng, X. (2001). Global vegetation root distribution for land modeling. *Journal of Hydrometeorology*, *2*, 525–530. https://doi.org/10.1175/1525-7541(2001)002<0525:GVRDFL>2.0.CO;2

Zhang, H., Li, J., Ying, Q., Yu, J. Z., Wu, D., Cheng, Y., et al. (2012). Source apportionment of PM2.5 nitrate and sulfate in China using a source-oriented chemical transport model. *Atmospheric Environment*, *62*, 228–242. https://doi.org/10.1016/j.atmosenv.2012.08.014

Zhang, L., & Zhou, T. (2015). Drought over East Asia: A review. *Journal of Climate*, *28*, 3375–3399. https://doi.org/10.1175/jcli-d-14-00259.1

Zhao, Z., Wang, Y., Qin, M., Hu, Y., Xie, Y., & Russell, A. G. (2019). Drought impacts on secondary organic aerosol: A case study in the southeast United States. *Environmental Science & Technology*, *53*, 242–250. https://doi.org/10.1021/acs.est.8b04842

Zheng, Y., Unger, N., Tadić, J. M., Seco, R., Guenther, A. B., Barkley, M. P., et al. (2017). Drought impacts on photosynthesis, isoprene emission and atmospheric formaldehyde in a mid-latitude forest. *Atmospheric Environment*, *167*, 190–201. https://doi.org/10.1016/j.atmosenv.2017.08.017